Evolution
November 2021, Volume 75 Issue 11 Pages 2898-2910
https://doi.org/10.1111/evo.14351
https://archimer.ifremer.fr/doc/00756/86797/

Distinct suites of pre- and post-adaptations indicate independent evolutionary pathways of snapping claws in the shrimp family Alpheidae (Decapoda: Caridea)

Chow Lai Him [1], De Grave Sammy [2], Anker Arthur [3], Poon Karina Ka Yan [1], Ma Ka Yan [1, 4], Chu Ka Hou [1], Chan Tin-Yam [5, 6], Tsang Ling Ming [1, *]

[1] Chinese Univ Hong Kong, Sch Life Sci, Simon FS Li Marine Sci Lab, Shatin, Hong Kong, Peoples R China.
[2] Univ Oxford, Museum Nat Hist, Parks Rd, Oxford, England.
[3] Univ Fed Goias, Inst Ciencias Biol ICB, Campus Samambaia,5 Ave Esperanca, Goiania, Go, Brazil.
[4] Sun Yat Sen Univ, Sch Ecol, Shenzhen, Peoples R China.
[5] Natl Taiwan Ocean Univ, Inst Marine Biol, Keelung, Taiwan.
[6] Natl Taiwan Ocean Univ, Ctr Excellence Oceans, Keelung, Taiwan.

* Corresponding author : Ling Ming Tsang, email address : lmtsang@cuhk.edu.hk

Abstract :

One of the most notable evolutionary innovations of marine invertebrates is the snapping claw of alpheid shrimps (Alpheidae), capable of generating a powerful water jet and a shock wave, used for defense, aggression, excavation, and communication. Evolutionary analysis of this character complex requires the study of a suite of complementary traits to discern pre-adaptations or post-adaptations of snapping behavior. A comprehensive phylogenetic analysis of the Alpheidae based on two mitochondrial and four nuclear markers, covering 107 species from 38 genera (77.6% generic coverage), is presented. Ancestral state reconstruction analyses revealed five independent origins of snapping, two of which relate to the morphologically similar but phylogenetically distant genera Alpheus and Synalpheus, highlighting significant convergence. The evolution of the five complementary traits (adhesive plaques, tooth-cavity system, dactylar joint type, chela size enlargement, and orbital hood) did not always show a significant correlation with the evolution of snapping overall, sometimes only in a few lineages, suggesting different evolutionary pathways were involved and demonstrating the versatility in the evolution of the snapping mechanisms.

Keywords : Convergent evolution, molecular phylogenetics, parallel evolution, snapping shrimp, systematics

Introduction

Key evolutionary innovations have contributed markedly to species diversification in a myriad of groups along the history of life by facilitating a shift in or expansion of adaptive zones (Heard and Hauser 1995; Vermeij 2006; Rabosky 2017). In decapod crustaceans, a number of such innovations have been recognised, including carcinisation (Morrison et al. 2002; Tsang et al. 2011), invasions of freshwater, cave and terrestrial habitats (Ashelby et al. 2012; von Rintelen et al. 2012), and infaunalisation (Carmona et al. 2004). Perhaps one of the most notable innovations in decapods is the evolution of snapping claws, which characterise the presently second largest family of Caridea, Alpheidae (Fig. 1), though paralleled by a few Palaemonidae genera (Anker et al. 2006a; Kaji et al. 2018)). Among the 750 or so currently recognised alpheid species in 49 genera, snapping claws are present in more than half of the species, most notably in the genera *Alpheus* (>300 species) and *Synalpheus* (>160 species). Their diversification, as well as the emergence of symbioses and eusociality in these two genera (Karplus 1987; Duffy 1996), are likely promoted by several functional significances of the snapping claws, including defence, predation, various intra- and interspecific interactions, rock boring and burrowing (e.g., MacGinitie 1937; Fischer and Meyer 1985; Schmitz and Herberholz 1998; Atkinson et al. 2003; Tóth and Duffy 2005). Elucidating the evolutionary pathway of snapping claws is, therefore, crucial to understanding the evolution of alpheid shrimps themselves.

Snapping refers to the extremely rapid claw closure, resulting, at least in some studied taxa (*Alpheus*), in ejection of a powerful water jet and production of a cavitation bubble, which implodes and generates an audible shock wave (Versluis et al. 2000). The ‘snap’ is used in various intra- and interspecific interactions, as well as communication in eusocial taxa (Tóth and Duffy

2005). The snapping process is controlled by multiple attributes of the chela, including size and applied closer muscle force (Versluis et al. 2000). It is therefore sensible to assume that the snapping mechanism is an evolutionary innovation and represents a character complex involving a set of functionally linked traits, collectively enabling a wholly new functioning appendage (Anker et al. 2006a). As part of parallel evolution, their adaptive relationship could be defined according to the evolutionary timing: 1) pre-adaptation in the common ancestor, 2) lineage-specific pre-adaptation and 3) post-adaptation. To obtain a comprehensive picture of the evolution of snapping, studying the evolution of complementary traits in concert are fundamental.

Four putative complementary traits related to snapping are 1) chela enlargement, 2) modification of the dactylar joint, 3) development of adhesive plaques on the chela, and 4) a tooth-cavity system on the cutting edge of the fingers. Chela size in Alpheidae shows huge variation from not enlarged at all to a size wider than the body and reaching half of the body length (Figs. 1, 2a). Supposing a certain threshold force is required for snapping, snapping taxa are expected to possess a relatively larger chela since chela size is correlated with muscle mass and closing force in other decapods (Levinton and Judge 1993; Claussen et al. 2008). Another trait related to force amplification is the type of dactylar joint (Fig. 2b), in which cocking joints distinctively possess latching and energy-storage mechanisms that allow ultrafast movement and eventually snapping (Kaji et al. 2018). In some snapping shrimps, cocking is further aided by exoskeletal structures called adhesive plaques, located on the distodorsal palm margin and the opposing dactylar base (Ritzmann 1973) (Fig. 2c). During cocking, the two plaques are held tightly by Stefan adhesion, resisting closing of the chela and thus allowing closer muscle to develop more tension (Ritzmann 1973). Finger armature plays a crucially important role in snapping and indeed many of the

snapping taxa exhibit a highly developed tooth-cavity system on the major claw, in the form of a large, plunger-like tooth on the dactylus fitting perfectly into a deep socket on the pollex. In less developed forms, this tooth-cavity system is represented by a small tooth fitting into a shallow depression or a broad bulge fitting into a deep groove; in rarer occasion, both fingers are armed with shallow fossae (Bruce 1988; Anker et al. 2006a; Anker 2019) (Fig. 2d). One additional complementary trait that is not directly related to claw specialisation is the development of the so-called orbital hood - an anterior projection of the carapace completely or partially covering the eyes. While the orbital hood is lacking in several 'lower' alpheid genera, the remaining groups show varying degrees of its development (Fig. 2e), which is speculated to provide some eye protection against the shrimp's own snaps or snaps from intraspecific encounters (Coutière 1899; Anker et al. 2006a).

Despite being a distinctive and ubiquitous group of crustaceans, the inter-generic relationships of Alpheidae remain understudied. The family-level morphological phylogeny of Anker et al. (2006a) remains the only comprehensive analysis performed to date, covering 56 species from all 36 genera known back then. They showed that at least some of the complementary traits were parallel pre-adaptations facilitating the evolution of snapping in alpheids, and discussed the two possible evolutionary scenarios for the evolution of the snapping claw in the family, i.e. single *versus* multiple origins. Previous molecular phylogenetic studies have been restricted to a few species-rich genera *Alpheus* (reviewed in Hurt et al. 2021) and *Synalpheus* (reviewed in Hultgren et al. 2014), as well as the *Betaeus* + *Betaeopsis* clade (Anker and Baeza 2014). A robust molecular phylogenetic framework is, therefore, required to corroborate the results of Anker et al. (2006a), due to high levels of homoplasy resulting in low support for some clades. We perfomed

the first molecular phylogenetic analysis of Alpheidae based on two mitochondrial and four nuclear DNA markers, covering 107 species from 38 genera. We aim to elucidate 1) the origin and evolutionary history of snapping claw and 2) the adaptive relationships between snapping and the five putatively complementary traits.

Materials and Methods

Sampling and DNA extraction, PCR and sequencing

A total of 107 alpheid species from 38 genera were included in this study (Table S1). Total genomic DNA was extracted from ethanol-preserved eggs, pleopods or pereiopods, using the QIAamp DNA Micro Kit (QIAGEN, Hilden, Germany) following the manufacturers' instructions. Partial fragments of two mitochondrial (12S, 16S rRNA) and four nuclear genes (histone 3 (H3), enolase (Enol), phosphoenolpyruvate carboxykinase (PEPCK), sodium-potassium ATPase α-subunit (NaK)) were amplified using the primers and protocols listed in Table S2. The PCR products were purified using the Millipore Montage PCR_{96} Cleanup Kit (Merck Millipore, Bi llerica, MA, USA) according to the manufacturer's instructions, or by the sequencing company (BGI, Shenzhen). Sequences were generated using the forward primer on an Applied Biosystems (ABI) 3700 automated sequencer using the ABI Big-dye Ready-Reaction Mix Kit (Life Technologies, Carlsbad), following the standard cycle sequencing protocol.

Phylogenetic Analyses

Sequences were aligned using MAFFT (Katoh and Standley 2013) or MUSCLE (Edgar 2004). Alignments of protein-coding genes (i.e., H3, Enol, PEPCK, NaK) were further confirmed by translating into amino acid sequences to ensure the absence of stop codons. Highly divergent

and poorly aligned regions of the 12S and 16S rRNA genes were trimmed using trimAl v1.3 (Capella-Gutiérrez et al. 2009) with a gap threshold of 20%. The best-fit substitution model for each marker, or each codon position for protein-coding genes was determined using PartitionFinder v2.1.1 (Lanfear et al. 2017), according to the corrected Akaike information criterion (AICc) (Table S3). The concatenated dataset was analysed under Maximum Likelihood (ML) with IQ-TREE v1.6.12 (Nguyen et al. 2015), and under Bayesian inference (BI) with MrBayes v3.2 (Ronquist et al. 2012). In the ML analysis, branch support was assessed by ultrafast bootstrapping (Minh et al. 2013) with 5,000 replicates. In the BI analysis, two independent Markov chain Monte Carlo (MCMC) runs of four chains were performed for 50 million generations, sampling every 50,000th generation. Convergence of chains was determined by having effective sample size (ESS) >200 for all parameters. One-fourth of the trees were discarded as burn-in. All trees were rooted by the outgroup species *Leander plumosus, Macrobrachium cf. tenuipes* and *Palaemon pacificus* (all Palaemonidae).

Ancestral state reconstruction

Ancestral states of the six traits (i.e., snapping behaviour, adhesive plaques, tooth-cavity system, dactylar joint, chela size and orbital hood) were assessed based on the ML topology with poorly resolved nodes (bootstrap value (BP) <85%) further collapsed using iTOL v4 (Letunic and Bork 2019) before the analysis.

Coding of the six traits was done on a species basis as listed in Table S4. Specifically for chela size, a proxy for interspecific comparison was calculated as $S = \frac{\sqrt{l \times w}}{cl}$, where l and w represent palm length and width, respectively (major cheliped if unequal), while cl represents

carapace length measured from the tip of the rostrum to the posterior margin of the carapace. Length information was retrieved from and averaged over accessible published records and specimens. For polymorphic and sexually dimorphic species, relative chela size was calculated separately for the two chela types or genders, respectively. For specimens of uncertain identity without cheliped information, relative chela size was shown as the range of all congeners, except for *Athanas* which has strong variation within genus and is not monophyletic in our phylogenetic analysis (see Results). For species without carapace length information, relative chela size was estimated from total length, if available. Given any potential intraspecific variation, interspecific variation in relative carapace length, as well as technical error, the ratios were arbitrarily grouped into five states of enlargement: non-enlarged ($S < 0.15$), slight ($0.15 \leq S < 0.30$), moderate ($0.30 \leq S < 0.45$), considerable ($0.45 \leq S < 0.60$) and great ($S \geq 0.60$). For orbital hood development, we slightly modified the definition by Anker et al. (2006a) and emphasised on the degree of eye coverage from the dorsal and lateral sides. Orbital hood was coded as 'absent' if eyes are largely exposed; 'incomplete' if the eyes are partly concealed dorsally (and laterally); 'complete' if the eyes are fully concealed dorsally and partly laterally; and 'perfect' if the eyes are fully concealed dorsally and laterally, and in many cases, also frontally.

The ancestral states were reconstructed per trait and for nodes at various taxonomic levels, using a Bayesian approach implemented in BayesTraits v3.0.1 (Pagel et al. 2004) with the 'MultiState' option. State transition was restricted to be stepwise in the analyses of the two continuously varying traits (i.e., chela size and orbital hood) by constraining the rate of non-stepwise transitions as zero. Exploratory reversible-jump MCMC (RJ-MCMC) analyses were first conducted to estimate the boundaries of the priors. Fifty million MCMC generations were run,

sampling every 5,000th generation, with an exponential hyperprior with the mean drawn from a uniform interval from 0 to 100, and automatic tuning for rate deviation to achieve an acceptance rate of 35%. First one-fourth of the generations were discarded as burn-in. Three independent runs were conducted in the formal analyses with the same parameters applied except with new, constrained priors. Stepping stones sampling (Xie et al. 2010) was performed to assess stationarity among chains via estimation of marginal likelihood (Kass and Raftery 1995) for each chain with 250 stones running for 5,000 iterations. Tracer v1.7 (Rambaut et al. 2018) was used to concatenate the three chains and obtain the mean posterior probabilities (PP) of the ancestral states, and mean and median transition rates. To elucidate the probable coevolutionary pathway of snapping and each of the morphological traits, ancestral state was re-analysed for each of the pairs as a compound trait. Transition was restricted to either shifting the state of snapping or the other trait in a stepwise manner. Transitions with 20-60% zero bin (Z) were considered non-critical to the model (Chow et al. 2021).

Testing of correlated trait evolution

Evolutionary covariation between snapping behaviour and each of the five morphological traits was tested using the threshold model implemented in the function 'threshBayes' of the R package phytools (Revell 2012). Since the analysis only allows binary coding for discrete traits, correlation between snapping and tooth-cavity system was only tested for taxa with a well-developed system. For the two continuously varying traits, states were converted into numerical pseudo-continuous data with respect to their degree of development, such that it ranged from one (i.e., the least developed state) to *K* (i.e., the total number of states, also the most developed). In addition, since chela size data included ranges of values, analyses were run twice with the

minimum and maximum values, respectively. The analyses were performed for the entire dataset, as well as trimmed datasets excluding snapping taxa from clade A or S, respectively (see Results), to detect any differentiated correlation signals. Two million MCMC generations were run, sampling every 1000th generation, with a burn-in of 20%. Convergence was assessed by the R package coda (Plummer et al. 2006) based on having ESS > 200. Additional generations were run if convergence was yet to be reached. Mean correlation coefficients (*r*) were retrieved and their significances were estimated from the absence of zero (i.e., no correlation) in the 95% highest posterior density (HPD) interval.

Results

Phylogeny of Alpheidae

The phylogenetic trees (Figs. 3, S1) were constructed based on a concatenated dataset comprising 2850 bp (16S: 544 bp, 12S: 563 bp, H3: 327 bp, Enol: 369 bp, PEPCK: 540 bp, NaK: 507 bp) with a mean missing rate of 4.9% of markers. The ML and BI trees were largely congruent in topology, but the former is better resolved at the deeper nodes; therefore our inference is mainly based on the ML tree. Seven of the genera were confirmed to be non-monophyletic (*Alpheopsis*, *Alpheus*, *Arete*, *Athanas*, *Automate*, *Leptalpheus*, *Salmoneus*). *Bannereus* was possibly paraphyletic with a divergent specimen of uncertain identity. *Metalpheus* was also potentially paraphyletic, but only supported in the BI analysis. The phylogeny of Alpheidae revealed a basal assemblage and two major clades: A and S, corresponding largely to the ‘higher alpheids’ following the annotation in Anker et al. (2006a) referring to the positions of the two largest genera, *Alpheus* and *Synalpheus*). Detailed results can be found in Supporting Information.

Evolution of snapping claw and related traits

Our ancestral state reconstruction analyses revealed six independent origins of snapping, originated in the most recent common ancestors (MRCA) of clades A-II, *Nennalpheus* (A-V), *Synalpheus* (clade S-II), and the two lineages of *Salmoneus* (clade S-III), respectively (PP = 1.00) (Fig. 4a). The presence of adhesive plaques was restricted to clades A-II, A-III, A-IV and A-V, encompassing three of the snapping lineages, with a single origin traced back to their MRCA (PP = 1.00) and two secondary losses within clade A-III (Fig. 4b). While the gain of snapping and adhesive plaques from the ancestral state proceeded in comparable rate, the latter promoted the former in a hierarchical fashion (Figs. 5a, S2). Once the derived state was attained, reversal in either trait was highly limited.

Well-developed tooth-cavity systems evolved independently in two of the snapping lineages: clades A-II and S-II (PP = 1.00) (Fig. 4c), with secondary reductions observed in the former clade. Weak tooth-cavity systems evolved three times, all within clade A, one of which involved one of the snapping lineages (clade A-V). The most probable coevolutionary pathway depicted is a gain of snapping behaviour followed by gain of tooth-cavity system, and subsequent shift among variants (Figs. 5b, S3).

Cocking pivot joint arose in the MRCA of clades A-II, A-III and A-IV (PP = 0.91), with a reversal to cocking slip joint at the root of clade A-IV (PP = 0.83), suggesting parallel evolution of cocking pivot joints (Fig. 4d). Gaining of snapping behaviour and cocking pivot joint from the ancestral state also occurred at comparable rates (Figs. 5c, S4). Subsequent transition to snapping in the presence of cocking pivot joint was also rapid, with reversal being negligible.

Alpheidae were likely derived from a common ancestor with moderately enlarged chela (PP = 0.88) and incomplete orbital hoods (PP = 0.64) (Fig. 4e, f). Chela size remained more or less similar (i.e., slightly to considerably enlarged) in most of the clades, but with at least four occurrences of size reduction (basal lineage IV, clades A-VI, S-III, S-IV) and five enlargement events (basal lineages I, II and III, clades A-I and S-V, as well as the snapping lineages of clades A-II and S-II) (Fig. 4e). In contrast, complete orbital hoods evolved early in the MRCA of basal lineage IV and higher Alpheidae (PP = 0.80) (Fig. 4f), and persisted until further independent development in six clades including four of the snapping lineages (clades A-I, A-II, A-III, A-VI, S-I, S-II, S-III) and reduction in clades S-III, S-IV and S-V. Changes among chela size categories in both the presence or absence of snapping proceeded at comparable rates, except that transition from ‘moderate’ to ‘considerable’ chela enlargement in snapping taxa was relatively restricted (Figs. 5d, S5). A similar pattern was observed for orbital hoods, but ‘perfect’ orbital hood represented an evolutionary endpoint for snapping taxa where reduction was limited (Figs. 5e, S6). Snapping gain likely occurred in taxa with ‘moderate’ or ‘considerable’ chela enlargement, but both transitions were not strongly supported in on our dataset, probably due to extensive variation within taxon such as sexual dimorphism. On the other hand, snapping gain was only evident for taxa with ‘complete’ orbital hood. While the evolutionary sequence of snapping and chela enlargement from the ancestral state was not clearly elucidated, our results suggest that snapping after orbital hood development, though further advances in orbital hoods, as well as chela size, also occurred after the evolution of snapping.

The evolution of a tooth-cavity system, chela size enlargement and orbital hoods in Alpheidae showed significant correlation with that of snapping behaviour (r ranged from 0.460–0.603) (Table S5). The correlation between the latter two traits and snapping was, however, not significant when considering snapping taxa of clade A or S only, except between snapping and chela size enlargement in clade S. Adhesive plaques and cocking pivot joint were evolutionarily significantly correlated with snapping only when considering snapping taxa of clade A (r = 0.483–0.574).

Discussion

Phylogeny of Alpheidae

Our molecular phylogeny of Alpheidae is generally in concordance with the previous morphological phylogeny (Anker et al. 2006a) at clade level, but with some significant discrepancies at intra-clade level. The alpheid diversification largely followed a single evolutionary pathway in the morphological phylogeny with the most highly derived and speciose genera concentrated in the crown, whereas our molecular analyses recovered at least two separate evolutionary pathways among the 'higher' genera. This suggests that most of the clades are faithfully characterised by morphological synapomorphies, but the presence of homoplasies and autapomorphies, may have caused conflict in the hypotheses at deeper levels. It is also important to mention that the morphological phylogeny of Anker et al. (2006a) contained only 36 genera out of 49 currently known ones, and therefore did not include several lineages or clades of phylogenetic importance, such as *Jengalpheops*, *Leslibetaeus*, *Pachelpheus* and *Richalpheus*.

In the primary taxonomic literature, the genera *Caligoneus*, *Coutieralpheus*, *Jengalpheops*, *Leslibetaeus*, *Potamalpheops*, *Stenalpheops* and *Yagerocaris* have been considered relatively basal, due to plesiomorphic features such as incomplete orbital hoods, a complete set of coxal mastigobranchs, unspecialised symmetrical chelipeds and presence of carpal brushes on the chelipeds. Our results, however, showed that only *Leslibetaeus* and *Yagerocaris* are resolved as 'basal', whilst the others assume relatively 'basal' positions among higher alpheids. *Automate*, *Bermudacaris* and *Coronalpheus* were found to accompany *Leslibetaeus*, whose relatively less derived status has already been hinted in Anker et al. (2006b). The enigmatic *Leslibetaeus*, which is morphologically quite distinct from all other alpheid genera, may represent a lineage that is perhaps closest to the MRCA of Alpheidae, since many of the 'basal' taxa in the derived clades superficially resemble *Leslibetaeus* rather than *Automate* and related genera (see below). The cave-dwelling *Yagerocaris*, originally misplaced in Hippolytidae (Kensley, 1988), was found to be a relict lineage without any particular phylogenetic affinity to other genera, supported by its combination of plesiomorphies and autapomorphies (Anker et al. 2006a; Anker 2008).

The evolutionary trend in clade A is hierarchically well-structured. The 'basal' genera *Jengalpheops* and *Pachelpheus* (clade A-VI) probably evolved from a *Leslibetaeus*-like ancestor, all showing similar frontal regions, and similarly shaped, small, symmetrical chelipeds. The recovery of *Metabetaeus* in the same clade is intriguing, since it shares little synapomorphies with other genera but generally agrees with its relatively less derivedstatus among higher alpheids, with a weak affinity to *Alpheopsis* (clade A-I). *Alpheopsis*, *Coutieralpheus*, *Prionalpheus* (clade A-I), *Parabetaeus* (clade A-IV) and *Nennalpheus* (clade A-V) belong to an intermediate group characterised by symmetrical chelipeds, moderately developed rostrum (sometimes reduced), and

296 the sixth pleurite with an articulated plate at the posteroventral angle (Anker et al. 2006a). However,
297 in the present phylogeny, *Bannereus* and *Vexillipar* were found embedded in clade A-I, whereas
298 *Parabetaeus* was recovered as sister to the leptalpheoid generic complex (*Leptalpheus* +
299 *Amphibetaeus* + *Fenneralpheus* + *Richalpheus*) (clade A-III), suggesting that the above grouping
300 is based largely on plesiomorphic features. The derived status of the leptalpheoid complex, as well
301 as *Alpheus* and allied genera (clade A-II), is generally concordant between molecular and
302 morphological analyses. Both clades possess moderately to greatly enlarged, asymmetrical
303 chelipeds, and in particular, a claw folding mechanism and peculiar armature of the fingers in in
304 the former clade (e.g., Anker et al. 2006a; Anker 2011), and a well-developed tooth-cavity system
305 in the latter clade (though maybe relatively weakly developed in some taxa).
306
307 The evolutionary trend of clade S is less obvious than that of clade A, since there was no
308 apparent 'basal' lineage revealed in the present study with incomplete generic coverage. *Betaeus*
309 and *Betaeopsis* (clade S-I) were suggested to be more related to the leptalpheoid genera (clade A-
310 III) based on morphological evidence (Anker et al. 2006a), but were herein recovered in a very
311 distant clade, more precisely as sister to *Synalpheus*. The highly specialised *Synalpheus* is
312 essentially the 'counterpart' of *Alpheus* of clade A. Both genera share greatly enlarged chela with
313 prominent tooth-cavity system and well-developed orbital hood, representing convergences in
314 snapping and eye protection related traits that led to their sister position in previous morphological
315 analysis (Anker et al. 2006a). They in fact differ in many other morphological aspects, including
316 details of the snapping claw (Coutière 1899; Banner and Banner 1975; Anker et al. 2006a),
317 reinforcing their separate origins as revealed in our analyses.
318

Caligoneus (clade S-III), *Stenalpheops* and *Potamalpheops* (clade S-IV) were considered as morphologically least derived genera (Anker et al. 2006a; Komai and Fujita, 2018), but the combination of their 'primitive' features may have resulted from secondary reductions and/or reversals. Mirroring the evolution of the leptalpheoid complex (clade A-III), asymmetrical chelipeds with a folding mechanism also evolved in the derived salmoneoid (clade S-III) and some members of the athanoid generic complexes (clade S-V), in a parallel evolution. The divergence of *Rugathanas* (clade S-IV) from the athanoid generic complex is surprising given their numerous morphological similarities (including many specific details, see Anker & Jeng 2007) but may be explained by its distinctive cheliped folding mechanism with the carpus excavated (*versus* merus in majority of other athanoid taxa) to accommodate the propodus. Nevertheless, a possible affinity between clade S-IV and the athanoid complex has been noted for *Stenalpheops* + *Potamalpheops* and *Pseudathanas*, however, based essentially on the features of the uropodal diaeresis (Miya 1997).

Evolution of snapping claws in Alpheidae

Snapping behaviour characterises essentially five alpheid genera, namely *Alpheus*, *Metalpheus*, *Pomagnathus*, *Racilius* (clade A-II) and *Synalpheus* (clade S-II) (Anker et al. 2006a), all with a single, powerful, major snapping claw with a well-developed plunger-fossa snapping mechanism. *Racilius* was confirmed to be nested within the paraphyletic *Alpheus*, while *Metalpheus* + *Pomagnathus* were also potentially embedded within *Alpheus* according to previous morphological and molecular analyses (Anker et al. 2006a; Hurt et al. 2021), but herein recovered as sister clade to *Alpheus* though. Nevertheless, in all analyses, these four genera belong at least in the same clade and snapping must have evolved in their MRCA. Snapping behaviour was also

more recently documented in *Nennalpheus* (with a cavity-cavity system on both chelae) and *Salmoneus* (able to produce only weak, barely audible snaps). Our analyses agree on the parallel evolution of snapping (Kaji et al. 2018), although the total number of origins herein recovered was higher, which may be attributed to uncertainty of snapping in several genera (*Alpheopsis*, *Amphibetaeus*, *Bannereus*, *Leptalpheus*, *Vexillipar*), as well as phylogenetic ambiguity. Should member of these five genera also snap, clade A might share a common snapping origin. On the other hand, snapping might have emerged only once in clade S-III since the hard polytomy might have imposed constraints on the ancestral state. On the basis of available evidence, snapping likely emerged at least four times in Alpheidae, more specifically, twice each in clade A and clade S, respectively.

Our results suggest that some of the putatively complementary traits show strong correlation with snapping in Alpheidae overall, whilst the remaining traits only show such correlation in one of the main clades, suggesting that different evolutionary pathways may have been involved. The evolution of snapping + adhesive plaques or dactylar joint type follows a bifurcating pathway, corresponding to clades A and S. The evolution of adhesive plaques and cocking pivot joints favoured the subsequent emergence of snapping in clade A, and thus the two characters are potential pre-adaptations, both related to enhancement of energy storage. The enlargement of adhesive plaques may further be a post-adaptation, which may have facilitated a greater diversification in the crown genus *Alpheus*. Nevertheless, the lack of parallel evolution of adhesive plaques in on our dataset indicates such adaptive relationship is not a requisite for the emergence of snapping. On the other hand, although cocking pivot joint had a single origin in Alpheidae, its precursor role may be reinforced by parallelism in Palaemonidae, especially

Periclimenaeus (Kaji et al. 2018). However, dactylar joint type may in fact be a complex trait itself, rendering the inference on the adaptive relationship rather coarse-grained. Cocking joints differ from non-cocking ones mainly by the presence of various dactylar retention mechanisms, one of which in cocking pivot joints is a set of two adhesive plaques (Kaji et al. 2018), which explains their largely synchronised evolution in Alpheidae. The second mechanism recognised, the functional subdivision of closer muscle and internal apodemes (Ritzmann 1974), is not only present in some taxa with cocking pivot joints, such as some *Alpheus* (clade A-II) and *Periclimenaeus* (Palaemonidae), but also in some with cocking slip joints, such as some *Salmoneus* (clade S-III) (Kaji et al. 2018). This replicated burst suggests a certain adaptive correlation, but further inference is hindered by the limited information about muscle mechanics across caridean shrimp in general. Despite this common feature, snapping alpheids of clades A and S clearly evolved snapping via two different pathways regarding the cocking system: that of clade A involved the transition to pivot joints with cocking aided by adhesive plaques (and in some cases, also by subdivided closer muscle and internal apodemes), while clade S retained slip joints but with structural changes such as muscle insertion angle to achieve cocking (Kaji et al. 2018).

Multiple evolutionary pathways are also evident in the evolution of the tooth-cavity system as a post-adaptation of snapping, but are not clade-defined as in the evolution of adhesive plaques and dactylar joint type. Our analysis shows that the evolution of snapping in the presence of tooth-cavity system or its variants is less supported than in the absence of such claw armature, despite the fact that they are frequently referred as the 'snapping mechanism'. From empirical observation, they are apparently not required for snapping, as exemplified by some *Salmoneus*, and several palaemonid genera with dentate cutting edge on the chela. Nevertheless, in several alpheid lineages,

388 including the two most speciose snapping clades (A-II, S-II), a perfect plunger-fossa system
389 evolved repeatedly, suggesting a functional advantage of this structure. The water jet produced
390 during snapping has been attributed to water displacement when the plunger is driven into the fossa
391 (Versluis et al. 2000), but as a post-adaptation, a tooth-cavity system is likely to help guide the
392 water jet trajectory and accelerate water flow, as there is a tapering channel through in front of the
393 cavity when the chela closes (Coutière 1899; Hess et al. 2013). A perfectly developed plunger-
394 fossa system is an extremely powerful weapon in various biotic interactions, and together with
395 additional ecological functions (e.g., boring into hard substrate), may explain the explosive
396 radiation observed in *Alpheus* and *Synalpheus*. The degree of development of tooth-cavity is highly
397 variable in *Alpheus* and, albeit to a much lesser degree, in *Synalpheus* (Banner & Banner 1975,
398 1982; Anker et al. 2006a). Therefore, one of the many remaining questions is the presence of
399 evolutionary hierarchy among tooth-cavity systems. Although a direction from weak to well-
400 developed tooth-cavity system is possible, such transition is not well supported by the present
401 results. Weak or imperfect tooth-cavity systems in other snapping lineages may in fact represent
402 cases of convergence.
403
404 Regarding chela size and orbital hood, alpheids are morphologically predisposed to the
405 evolution of snapping. In cocking joints, the closing force of the claw is not simply proportional
406 to muscle mass and claw size, but related to the proportion of closer muscle contributing to energy
407 storage (Kaji et al. 2018), The presence of cocking aids may further liberate any constraints on
408 snapping claw size. This is essentially why it is possible for taxa with relatively small chela to
409 snap. However, our results suggest that 'moderately' enlarged chela represents a minimally
410 required size with reduction not documented after snapping emerged. This degree of enlargement

411 probably was already present since its divergence, though the initial selection forces remain
412 enigmatic. Further chela enlargement did occur in non-snapping lineages (Fig. 1b, d) but
413 apparently did not favour the subsequent evolution of snapping. In contrast, after the emergence
414 of snapping, there is a tendency towards further post-adaptive chela enlargement . This may be
415 attributed to the consistent selection towards stronger snaps since chela size is correlated with
416 water jet velocity and distance (Herberholz and Schmitz 1999). Although the evolutionary trend
417 of chela size, as well as its adaptive relationship with snapping in Palaemonidae remain unknown
418 and is out of scope of this study, it is an unlikely evolutionary coincidence that the only two
419 caridean families with greatly enlarged chelipeds evolved snapping. In contrast to the single
420 evolutionary pathway towards chela enlargement, the evolution of snapping + orbital hood is
421 relatively more flexible in Alpheidae, despite the advancement of orbital hood from 'incomplete'
422 to 'complete' being consistently a prerequisite. In some of the snapping lineages, snapping gain is
423 followed by the advancement of orbital hood to 'perfect', concurring with the long hypothesised
424 concerted evolution (Coutière 1899; Anker et al. 2006a). Interestingly, these lineages (i.e., *Alpheus*
425 and *Synalpheus*) also produce the strongest snaps, due to the presence of well-developed tooth-
426 cavity systems and/or 'considerably' to 'greatly' enlarged chela, as well as adhesive plaques in
427 *Alpheus*, supporting the hypothesis that protection from snaps is one of the main functional
428 significances of orbital hoods (Coutière 1899; Anker et al. 2006a). However, orbital hoods are
429 certainly not a strict prerequisite of snapping, since this structure is unique to Alpheidae, whilst
430 snapping lineages also evolved within Palaemonidae without formation of orbital hoods.
431 Nevertheless, this feature may have facilitated evolution of snapping in alpheid shrimps by
432 relieving evolutionary constraints from potential injuries associated with intraspecific encounters.
433 This may be supported by the much higher diversity of snapping taxa, the greater number of

434 independent origins of snapping, and the stronger attainable snap (Kaji et al. 2018) in Alpheidae
435 than in Palaemonidae. This leaves a question what drove orbital hood reduction in Alpheidae under
436 the presence or absence of snapping behaviour, in the present phylogenetic hypothesis. Insights
437 may be gained from investigations on the other functions of orbital hood using, for example,
438 *Betaeus* with well-developed orbital hood as positive models, and the athanoid generic complex
439 with prevalent orbital hood reduction as negative models.
440
441 In summary, the ancestral development of orbital hood and chela enlargement set the stage
442 for the evolution of snapping in alpheid shrimps. The emergence of snapping claws represents a
443 convergence in the two main snapping lineages with different mechanisms adopted to cross the
444 energy threshold. Clade A evolved pre-adaptive adhesive plaques and pivot dactylar joint, while
445 clade S had modifications in muscle dynamics. Post-adaptive development of tooth-cavity systems
446 and further chela enlargement subsequently improved snapping performance in both lineages in
447 parallel, allowing more powerful snaps and leading to a significantly greater diversification in
448 *Alpheus* (clade A-II) and *Synalpheus* (clade S-II) compared to other snapping and non-snapping
449 genera. As snaps became stronger, orbital hood advanced as post-adaptation in tandem to provide
450 additional eye protection from forceful chela closure. The independent evolutionary pathways of
451 snapping claws with distinct suites of pre- and post-adaptations demonstrate the versatility in the
452 evolution of this character complex.

Literature cited

Anker, A. 2008. A worldwide review of stygobiotic and stygophilic shrimps of the family Alpheidae (Crustacea, Decapoda, Caridea). Subterr. Biol. 6:1–16.

Anker, A. 2011. Six new species and three new records of infaunal alpheid shrimps from the genera *Leptalpheus* Williams, 1965 and *Fenneralpheus* Felder & Manning, 1986 (Crustacea, Decapoda). Zootaxa 3041:1–38.

Anker, A. 2019. The alpheid shrimp genus *Nennalpheus* Banner & Banner, 1981 in the tropical eastern Atlantic, with description of a new species from Gabon and new records of *N. sibogae* (De Man, 1910) in the Indo-West Pacific (Malacostraca: Decapoda: Caridea). Zootaxa 4646:87–100.

Anker, A., S. T. Ahyong, P. Y. Noel, and A. R. Palmer. 2006a. Morphological phylogeny of alpheid shrimps: parallel preadaptation and the origin of a key morphological innovation, the snapping claw. Evolution 60:2507–2528.

Anker, A., D. Poddoubtchenko, and I. S. Wehrtmann. 2006b. *Leslibetaeus coibita*, n. gen., n. sp., a new alpheid shrimp from the Pacific coast of Panama (Crustacea: Decapoda). Zootaxa 1183:27–41.

Anker, A., and J. A. Baeza. 2014. Molecular and morphological phylogeny of hooded shrimps, genera *Betaeus* and *Betaeopsis* (Decapoda, Alpheidae): testing the center of origin biogeographic model and evolution of life history traits. Mol. Phylogenet. Evol. 64:401–415.

Anker, A., and M-S. Jeng. 2007. Establishment of a new genus for *Arete borradailei* Coutière, 1903 and *Athanas verrucosus* Banner and Banner, 1960, with redefinitions of *Arete* Stimpson, 1860 and *Athanas* Leach, 1814 (Crustacea: Decapoda: Alpheidae). Zool. Stud. 46:454–472.

476 Ashelby, C. W., T. J. Page, S. De Grave, J. M. Hughes, and M. L. Johnson. 2012. Regional scale
477 speciation reveals multiple invasions of freshwater in Palaemoninae (Decapoda). Zool. Scr.
478 41:293–306.
479 Atkinson, R. J. A., M. E. Gramitto, and C. Froglia. 2003. Aspects of the biology of the
480 burrowing shrimp *Alpheus glaber* (Olivi) (Decapoda: Caridea: Alpheidae) from the Central
481 Adriatic. Ophelia 57:27–42.
482 Banner, D. M., and A. H. Banner. 1975. The alpheid shrimp of Australia. Part 2: the genus
483 *Synalpheus*. Rec. Aust. Mus. 29:267–389.
484 Banner, D. M., and A. H. Banner. 1982. The alpheid shrimp of Australia. Part III: the remaining
485 alpheids, principally the genus *Alpheus*, and the family Ogyrididae. Rec. Aust. Mus. 34:1–
486 357.
487 Bruce, A. J. 1988. *Bannereus anomalus*, new genus, new species, a deep-sea alpheid shrimp
488 from the Coral Sea. Pac. Sci.42:139–149.
489 Capella-Gutiérrez, S., J. M. Silla-Martínez, and T. Gabaldón. 2009. trimAl: a tool for automated
490 alignment trimming in large-scale phylogenetic analyses. Bioinformatics 25:1972–1973.
491 Carmona, N. B., L. A. Buatois, and M. G. Mángano. 2004. The trace fossil record of burrowing
492 decapod crustaceans: evaluating evolutionary radiations and behavioural convergence. Foss.
493 Strat. 51:141–153.
494 Chow, L. H., S. De Grave, and L. M. Tsang. 2021. Evolution of protective symbiosis in
495 palaemonid shrimps (Decapoda: Caridea) with emphases on host spectrum and
496 morphological adaptations. Mol. Phylogenet. Evol. 162:107201.

497 Claussen, D. L., G. W. Gerald, J. E. Kotcher, and C. A. Miskell. 2008. Pinching forces in
498 crayfish and fiddler crabs, and comparisons with the closing forces of other animals. J.
499 Comp. Physiol. B 178:333–342.
500 Coutière, H. (1899). Les Alpheidae, morphologie externe et interne, formes larvaires, bionomie.
501 Ann. Sci. Nat., Zool. Paléontol., Série 8 9:1–559.
502 Duffy, J. E. 1996. Eusociality in a coral-reef shrimp. Nature 381:512–514.
503 Edgar, R. C. 2004. MUSCLE: Multiple sequence alignment with high accuracy and high
504 throughput. Nucleic Acids Res. 32:1792–1797.
505 Fischer, R., and W. Meyer. 1985. Observations on rock boring by *Alpheus saxidomus*
506 (Crustacea: Alpheidae). Mar. Biol. 89:213–219.
507 Heard, S. B., and D. L. Hauser. 1995. Key evolutionary innovations and their ecological
508 mechanisms. Historical Biol. 10:151–173.
509 Herberholz, J., and B. Schmitz. 1999. Flow visualisation and high speed video analysis of water
510 jets in the snapping shrimp. J. Comp. Physiol. A 185:41–49.Hess, D., C. Brücker, F. Hegner,
511 A. Balmert, and H. Bleckmann. 2013. Vortex formation with a snapping shrimp claw. PLoS
512 One 8:e77120.
513 Hultgren, K. M., C. Hurt, and A. Anker. 2014. Phylogenetic relationships within the snapping
514 shrimp genus *Synalpheus* (Decapoda: Alpheidae). Mol. Phylogenet. Evol. 77:116–125.
515 Hurt, C., K. Hultgren, A. Anker, A. R. Lemmon, E. M. Lemmon, and H. Bracken-Grissom.
516 2021. First worldwide molecular phylogeny of the morphologically and ecologically
517 hyperdiversified snapping shrimp genus *Alpheus* (Malacostraca: Decapoda). Mol.
518 Phylogenet. Evol. 158:107080.

519 Kaji, T., A. Anker, C. S. Wirkner, and A. R. Palmer. 2018. Parallel saltational evolution of
520 ultrafast movements in snapping shrimp claws. Curr. Biol. 28:106–113.
521 Karplus, I. 1987. The association between gobiid fishes and burrowing alpheid shrimps.
522 Oceanogr. Mar. Biol. Ann. Rev. 25:507–562.
523 Kass, R. E., and A. E. Raftery. 1995. Bayes factors. J. Am. Stat. Assoc. 90:773–795.
524 Katoh, K., and D. M. Standley. 2013. MAFFT multiple sequence alignment software version 7:
525 improvements in performance and usability. Mol. Biol. Evol. 30:772–780.
526 Kensley, B. 1988. New species and records of cave shrimps from the Yucatan Peninsula
527 (Decapoda: Agostocarididae and Hippolytidae). J. Crustac. Biol. 8:688–699.
528 Komai, T., and Y. Fujita. 2018. A new genus and new species of alpheid shrimp from a marine
529 cave in the Ryukyu Islands, Japan, with additional record of *Salmoneus antricola* Komai,
530 Yamada Yunokawa, 2015 (Crustacea: Decapoda: Caridea). Zootaxa 4369:575–586.
531 Lanfear, R., P. B. Frandsen, A. M. Wright, T. Senfeld, and B. Calcott. 2017. PartitionFinder 2:
532 new methods for selecting partitioned models of evolution for molecular and morphological
533 phylogenetic analyses. Mol. Biol. Evol. 34:772–773.
534 Letunic, I., and P. Bork. 2019. Interactive Tree Of Life (iTOL) v4: recent updates and new
535 developments. Nucleic Acids Res. 47:W256–W259.
536 Levinton, J. S., and M. L. Judge. 1993. The relationship of closing force to body size for the
537 major claw of *Uca pugnax*. Funct. Ecol. 7:339–345.
538 MacGinitie, G. E. 1937. Notes on the natural history of several marine Crustacea. Am. Midl.
539 Nat. 18:1031–1037.
540 Minh, B. Q., M. A. T. Nguyen, and A. von Haeseler. 2013. Ultrafast approximation for
541 phylogenetic bootstrap. Mol. Biol. Evol. 30:1188–1195.

Miya, Y. 1997. *Stenalpheops anacanthus*, new genus, new species (Crustacea, Decapoda, Alpheidae) from the Seto Inland Sea and the Sea of Ariake, South Japan. Bull. Faculty of Liberal Arts, Nagasaki Univ. 38:145–161.

Morrison, C. L., A. W. Harvey, S. Lavery, K. Tieu, Y. Huang, and C. W. Cunningham. 2002. Mitochondrial gene rearrangements confirm the parallel evolution of the crab-like form. Proc. R. Soc. B 269:345–350.

Nguyen, L., H. A. Schmidt, A. von Haeseler, and B. Q. Minh. 2015. IQ-TREE: a fast and effective stochastic algorithm for estimating maximum-likelihood phylogenies. Mol. Biol. Evol. 32:268–274.

Pagel, M., A. Meade, and D. Barker. 2004. Bayesian estimation of ancestral character states on phylogenies. Syst. Biol. 53:673–684.

Plummer, M., N. Best, K. Cowles, and K. Vines. 2006. CODA: convergence diagnosis and output analysis for MCMC. R News 6:7–11.

Rabosky, D. L. 2017. Phylogenetic tests for evolutionary innovation: the problematic link between key innovations and exceptional diversification. Philos. Trans. R. Soc. Lond. B 372:20160417.

Rambaut, A., A. J. Drummond, D. Xie, G. Baele, and M. A. Suchard. 2018. Posterior summarization in Bayesian phylogenetics using Tracer 1.7. Syst. Biol. 67:901–904.

Revell, L. J. 2012. phytools: an R package for phylogenetic comparative biology (and other things). Methods Ecol. Evol. 3:217–223.

Ritzmann, R. 1973. Snapping behavior of the shrimp *Alpheus californiensis*. Science 181:459–460.

564 Ritzmann, R. 1974. Mechanisms for the snapping behaviour of two alpheid shrimp, *Alpheus*
565 *californiensis* and *Alpheus heterochelis*. J. Comp. Physiol. 95:217–236.
566 Ronquist, F., M. Teslenko, P. van der Mark, D. L. Ayres, A. Darling, S. Höhna, B. Larget, L.
567 Liu, M. A. Suchard, and J. P. Huelsenbeck. 2012. MrBayes 3.2: efficient Bayesian
568 phylogenetic inference and model choice across a large model space. Syst. Biol. 61:539–
569 542.
570 Schmitz, B., and J. Herberholz. 1998. Snapping behaviour in intraspecific agonistic encounters in
571 the snapping shrimp. J. Biosci. 23:623–632.
572 Tóth, E., and J. E. Duffy. 2005. Coordinated group response to nest intruders in social shrimp.
573 Biol. Lett. 1:49–52.
574 Tsang, L. M., T. Y. Chan, S. T. Ahyong, and K. H. Chu. 2011. Hermit to king, or hermit to all:
575 multiple transitions to crab-like forms from hermit crab ancestors. Syst. Biol. 60:616–629.
576 Vermeij, G. J. 2006. Historical contingency and the purported uniqueness of evolutionary
577 innovations. Proc. Natl. Acad. Sci. USA 103:1804–1809.
578 Versluis, M., B. Schmitz, A. von der Heydt, and D. Lohse. 2000. How snapping shrimp snap:
579 through cavitating bubbles. Science 289:2114–2117.
580 von Rintelen, K., T. J. Page, Y. Cai, K. Roe, B. Stelbrink, B. R. Kuhajda, T. M. Iliffe, J. Hughes,
581 and T. von Rintelen. 2012. Drawn to the dark side: a molecular phylogeny of freshwater
582 shrimps (Crustacea: Decapoda: Caridea: Atyidae) reveals frequent cave invasions and
583 challenges current taxonomic hypotheses. Mol. Phylogenet. Evol. 63:82–96.
584 Xie, W., P. O. Lewis, Y. Fan, L. Kuo, and M. H. Chen. 2010. Improving marginal likelihood
585 estimation for Bayesian phylogenetic model selection. Syst. Biol. 60:150–160.

Figure legends

Figure 1. Eight species from eight representative genera of the family Alpheidae, showing the diversity of cheliped size and shape: a) *Jengalpheops rufus* Anker & Dworschak, 2007, b) *Automate cf. dolichognatha* (De Man, 1888), c) *Alpheopsis cf. yaldwyni* Banner & Banner, 1973, d) *Aretopsis amabilis* De Man, 1910, e) *Athanas japonicus* Kubo, 1936, f) *Betaeus granulimanus* Yokoya, 1927, g) *Alpheus barbatus* Coutière, 1897, and h) *Synalpheus streptodactylus* Coutière, 1905. (a-f) non-snapping species, (g, h) snapping species. Photographs by Tin-Yam Chan from expeditions organised by the Muséum national d'Histoire naturelle, Paris (a-d, g, h) and Lai Him Chow (e, f).

Figure 2. Illustrations of the five complementary traits of snapping: a) chela size, b) dactylar joint type, c) adhesive plaques, d) tooth-fossa system, and e) orbital hood. Figures redrawn after various sources.

Figure 3. Phylogenetic tree of Alpheidae resolved by maximum likelihood. Branch support values (BP/PP) are indicated as percentages, those with both values < 85% are not shown. Major lineages or clades, and genera are highlighted.

Figure 4. Ancestral state reconstruction of six traits of Alpheidae: a) snapping, b) adhesive plaques, c) tooth-fossa system, d) dactylar joint type, e) chela size enlargement, and f) orbital hood. Branch colour represents the most probable state (only the most developed states for chela size are

608 indicated while the least developed states are shown as dots at tips). Posterior probabilities of
609 ancestral states are indicated for selected nodes in the form of pie charts.
610
611 Figure 5. Coevolutionary pathways of snapping and corresponding traits: a) adhesive plaques, b)
612 tooth-fossa system, c) dactylar joint, d) chela size enlargement, and e) orbital hood. Stars indicate
613 the ancestral state of Alpheidae revealed by ancestral state reconstruction analyses. Arrows
614 between states represent the direction of transition, with sizes being proportional to the normalised
615 median rate as indicated. Arrow colour represents the state being shifted to, except that black and
616 white depict reversals and transitions not critical to the model (Z = 20–60%), respectively.
617 Transitions with median rate of zero are not shown. The most probable and less probable
618 evolutionary pathways are illustrated by solid-line and dotted-line arrows, respectively. Crosses
619 on dotted-line arrows indicate further transition is not supported (i.e., zero median rate).

A

B

C

D

E

F

G

H

Non-snapping

Snapping

A Chela size

Non-enlarged

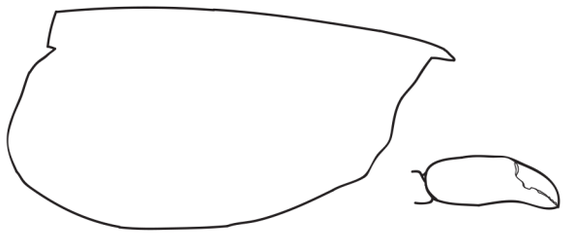

Slightly enlarged

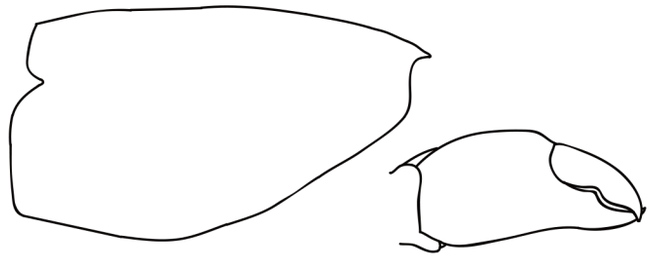

Moderately enlarged

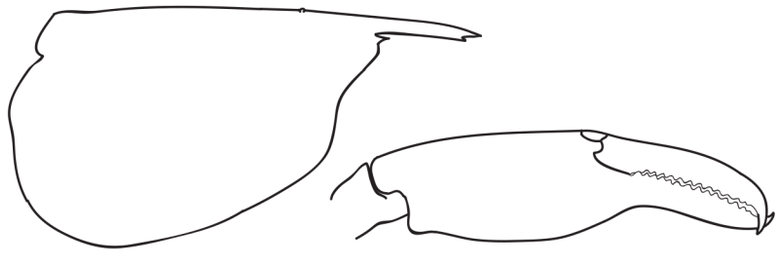

Considerably enlarged

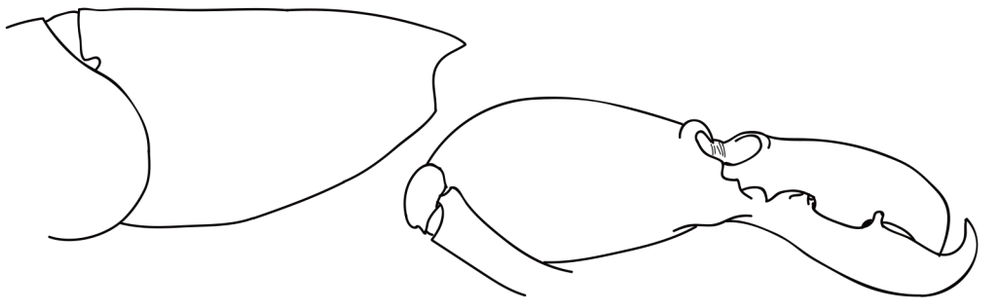

Greatly enlarged

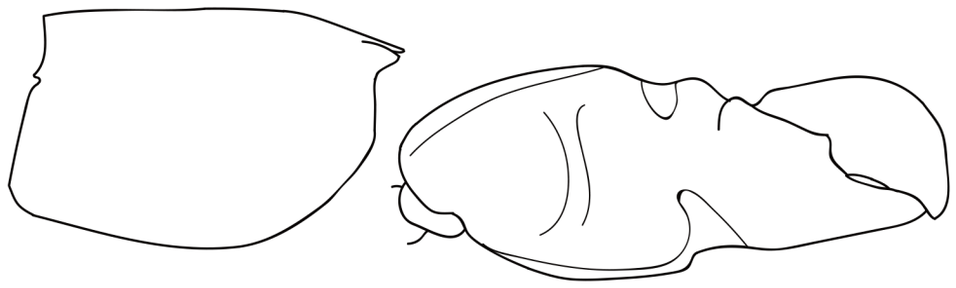

B Dactylar joint

(Cocking) Pivot joint

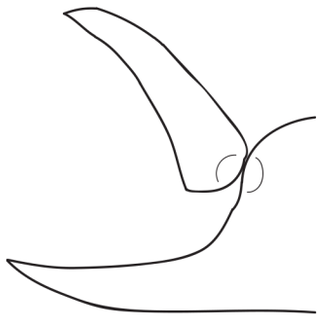

(Cocking) Slip joint

C Adhesive plaque (AP)

With AP

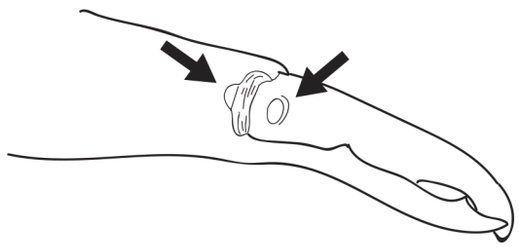

Without AP

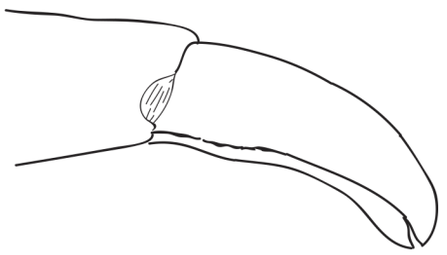

D Tooth-cavity (TC) or Cavity-cavity (CC) system

Without TC

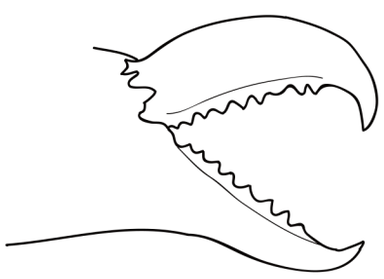

With weak TC

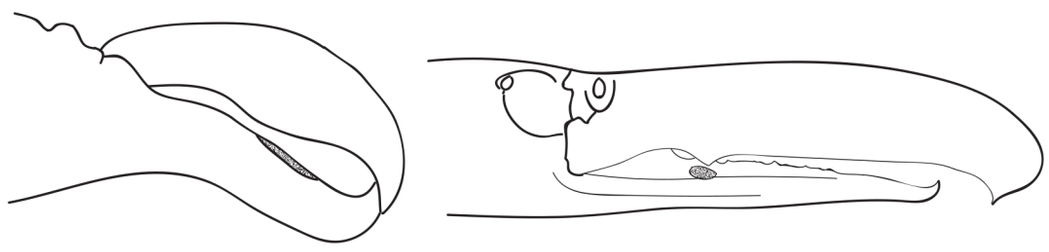

With TC

With CC

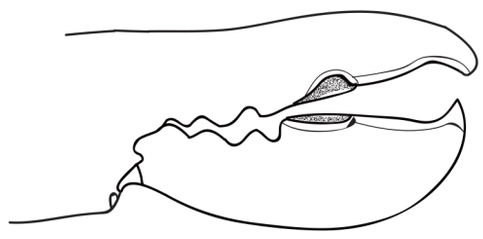

E Orbital hood

Absent

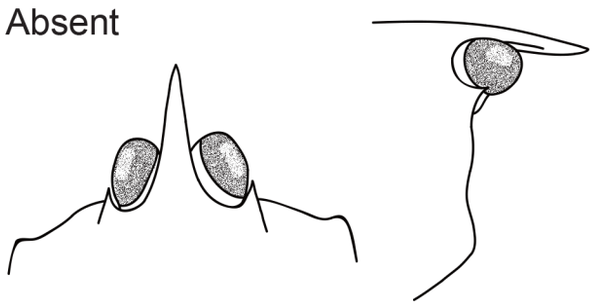

Incomplete

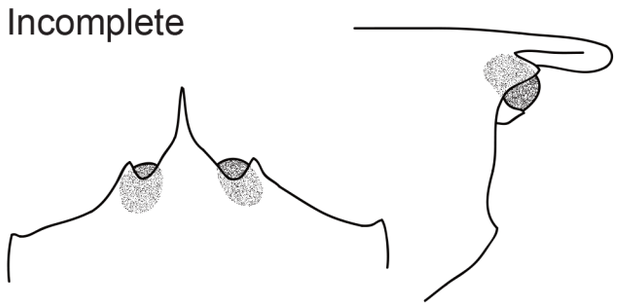

Complete

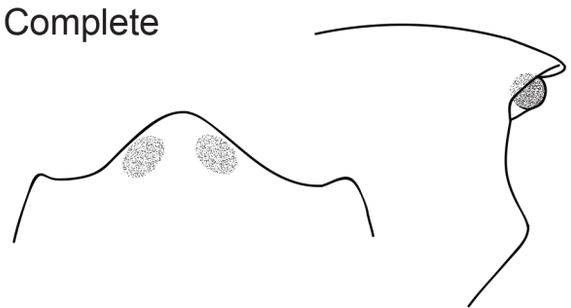

Perfect

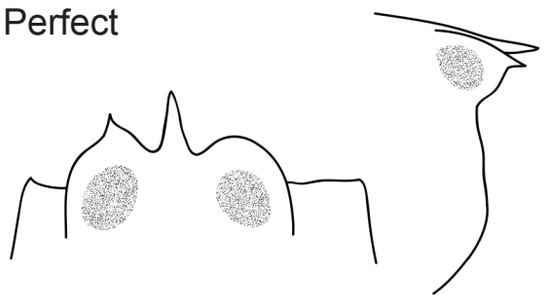

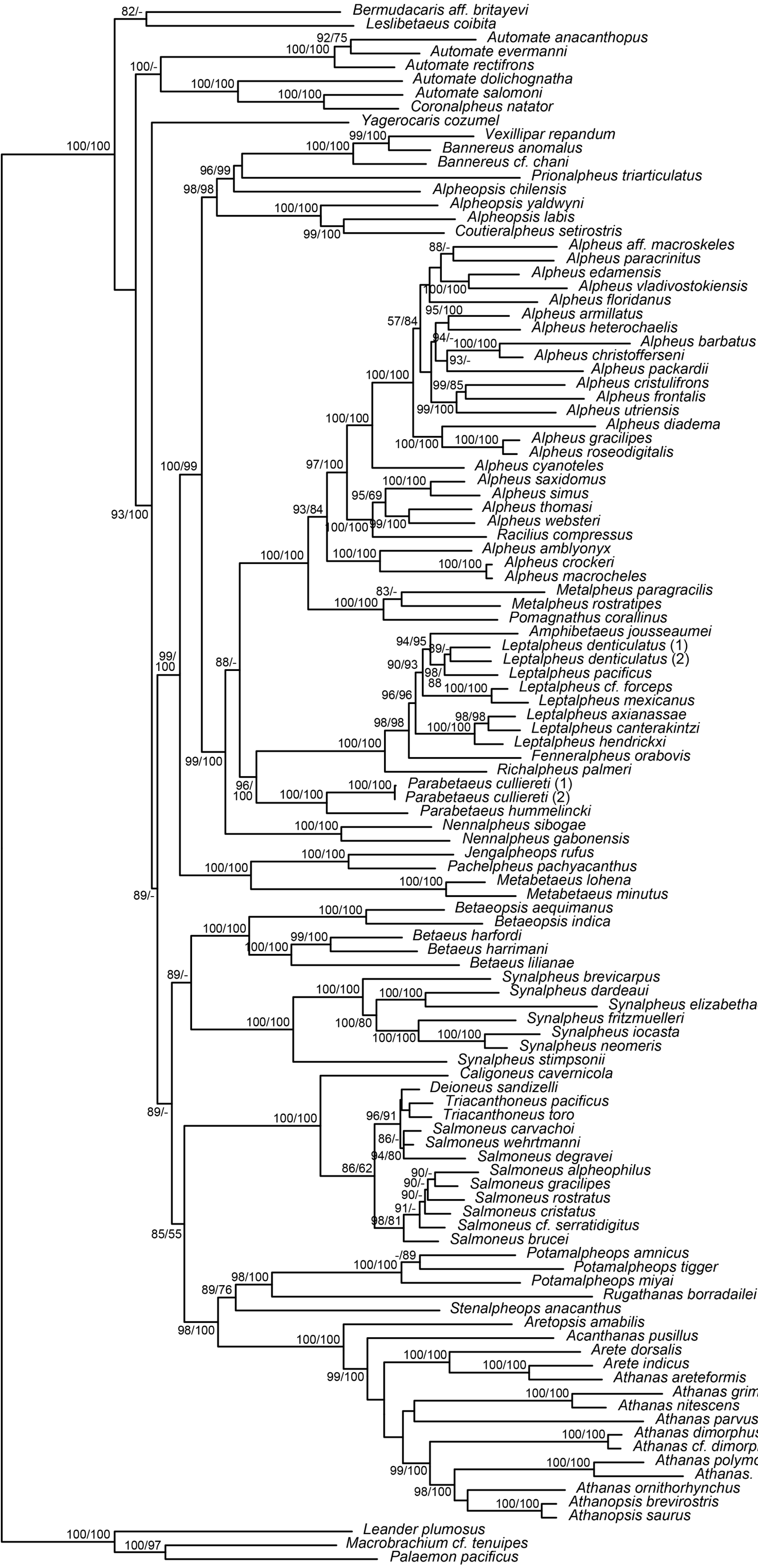
Bermudacaris aff. britayevi
Leslibetaeus coibita
Automate anacanthopus
Automate evermanni
Automate rectifrons
Automate dolichognatha
Automate salomoni
Coronalpheus natator
Yagerocaris cozumel
Vexillipar repandum
Bannereus anomalus
Bannereus cf. chani
Prionalpheus triarticulatus
Alpheopsis chilensis
Alpheopsis yaldwyni
Alpheopsis labis
Coutieralpheus setirostris
Alpheus aff. macroskeles
Alpheus paracrinitus
Alpheus edamensis
Alpheus vladivostokiensis
Alpheus floridanus
Alpheus armillatus
Alpheus heterochaelis
Alpheus barbatus
Alpheus christofferseni
Alpheus packardii
Alpheus cristulifrons
Alpheus frontalis
Alpheus utriensis
Alpheus diadema
Alpheus gracilipes
Alpheus roseodigitalis
Alpheus cyanoteles
Alpheus saxidomus
Alpheus simus
Alpheus thomasi
Alpheus websteri
Racilius compressus
Alpheus amblyonyx
Alpheus crockeri
Alpheus macrocheles
Metalpheus paragracilis
Metalpheus rostratipes
Pomagnathus corallinus
Amphibetaeus jousseaumei
Leptalpheus denticulatus (1)
Leptalpheus denticulatus (2)
Leptalpheus pacificus
Leptalpheus cf. forceps
Leptalpheus mexicanus
Leptalpheus axianassae
Leptalpheus canterakintzi
Leptalpheus hendrickxi
Fenneralpheus orabovis
Richalpheus palmeri
Parabetaeus cullierei (1)
Parabetaeus cullierei (2)
Parabetaeus hummelincki
Nennalpheus sibogae
Nennalpheus gabonensis
Jengalpheops rufus
Pachelpheus pachyacanthus
Metabetaeus lohena
Metabetaeus minutus
Betaeopsis aequimanus
Betaeopsis indica
Betaeus harfordi
Betaeus harrimani
Betaeus lilianae
Synalpheus brevicarpus
Synalpheus dardeaui
Synalpheus elizabethae
Synalpheus fritzmuelleri
Synalpheus iocasta
Synalpheus neomeris
Synalpheus stimpsonii
Caligoneus cavernicola
Deioneus sandizelli
Triacanthoneus pacificus
Triacanthoneus toro
Salmoneus carvachoi
Salmoneus wehrtmanni
Salmoneus degravei
Salmoneus alpheophilus
Salmoneus gracilipes
Salmoneus rostratus
Salmoneus cristatus
Salmoneus cf. serratidigitus
Salmoneus brucei
Potamalpheops amnicus
Potamalpheops tigger
Potamalpheops miyai
Rugathanas borradailei
Stenalpheops anacanthus
Aretopsis amabilis
Acanthanas pusillus
Arete dorsalis
Arete indicus
Athanas areteformis
Athanas grimaldii
Athanas nitescens
Athanas parvus
Athanas dimorphus
Athanas cf. dimorphus
Athanas polymorphus
Athanas. cf. japonicus
Athanas ornithorhynchus
Athanopsis brevirostris
Athanopsis saurus
Leander plumosus
Macrobrachium cf. tenuipes
Palaemon pacificus
0.16
Basal
Higher Alpheidae I (Clade A)
Higher Alpheidae II (Clade S)
Outgroup
Bermudacaris
Leslibetaeus
Automate
Coronalpheus
Yagerocaris
Vexillipar
Bannereus
Prionalpheus
Alpheopsis
Coutieralpheus
Alpheus I
Racilius
Alpheus II
Metalpheus
Pomagnathus
Amphibetaeus
Leptalpheus
Fenneralpheus
Richalpheus
Parabetaeus
Nennalpheus
Jengalpheops
Pachelpheus
Metabetaeus
Betaeopsis
Betaeus
Synalpheus
Caligoneus
Deioneus
Triacanthoneus
Salmoneus
Potamalpheops
Rugathanas
Stenalpheops
Aretopsis
Acanthanas
Arete
Athanas
Athanopsis

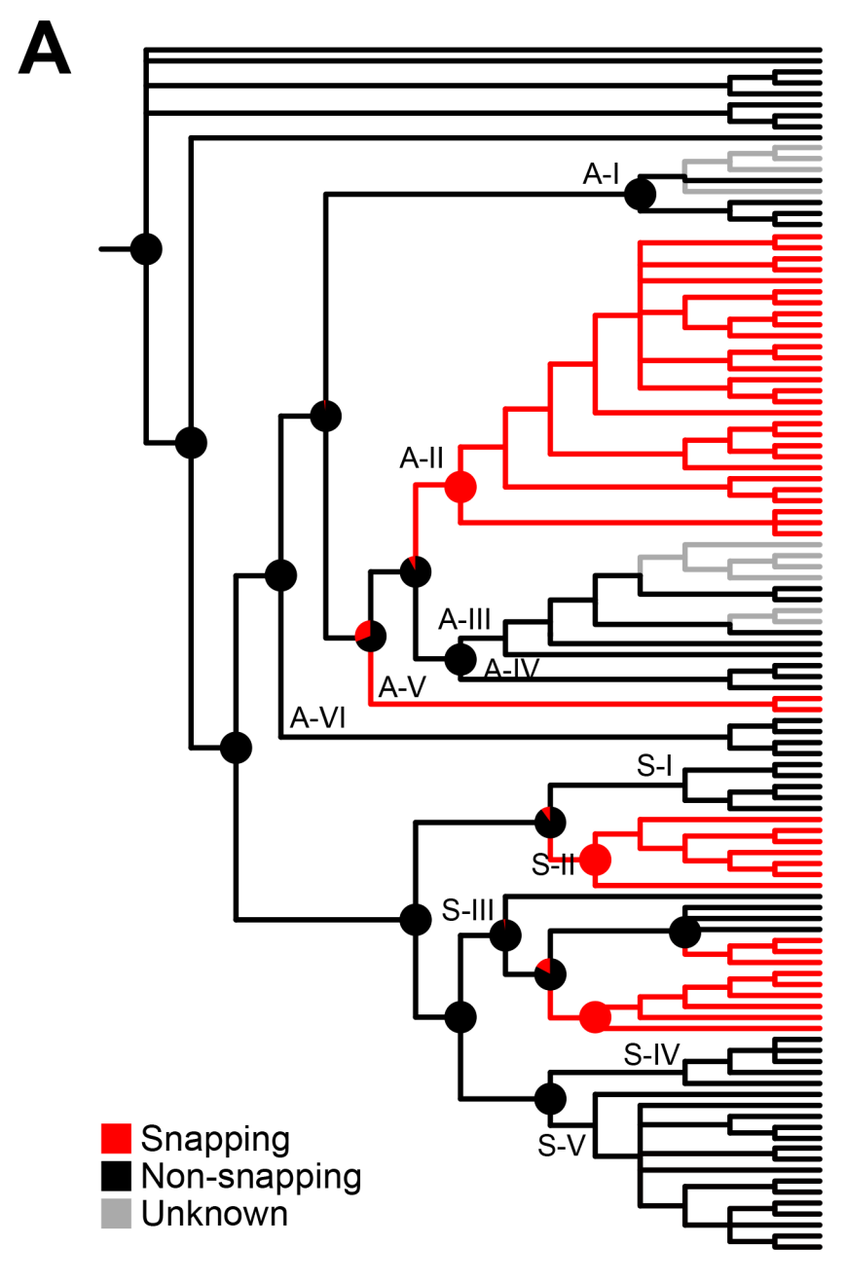
A
A-I
A-II
A-III
A-IV
A-V
A-VI
S-I
S-II
S-III
S-IV
S-V
Snapping
Non-snapping
Unknown

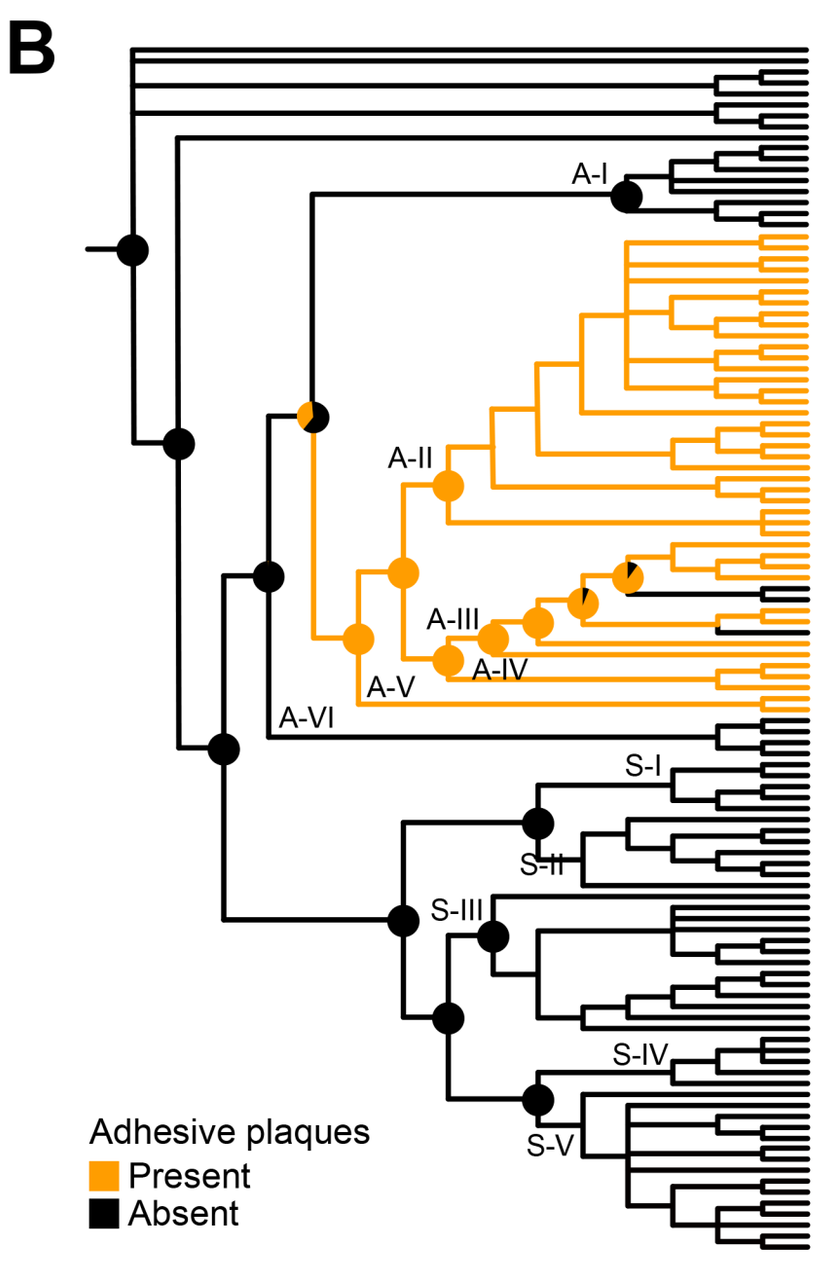
B
A-I
A-II
A-III
A-IV
A-V
A-VI
S-I
S-II
S-III
S-IV
S-V
Adhesive plaques
Present
Absent

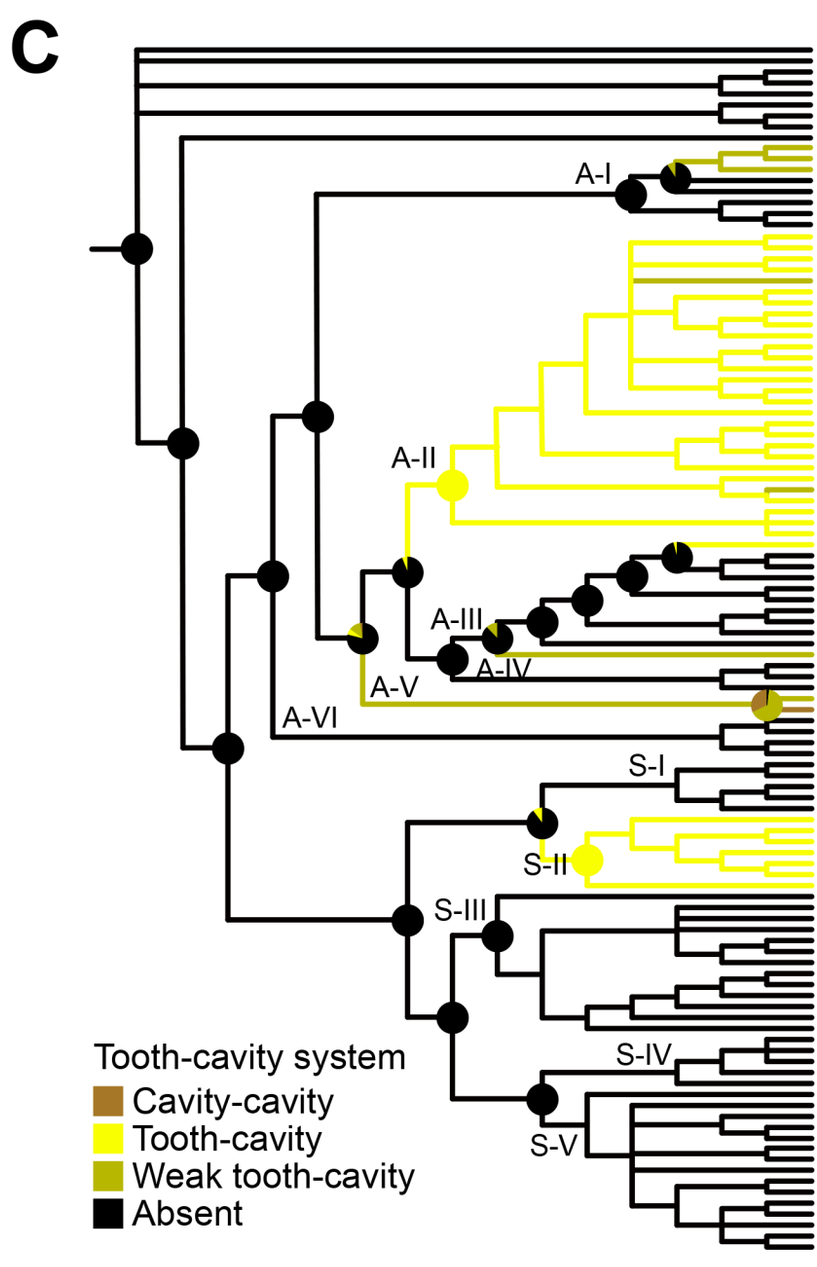
C
A-I
A-II
A-III
A-IV
A-V
A-VI
S-I
S-II
S-III
S-IV
S-V
Tooth-cavity system
Cavity-cavity
Tooth-cavity
Weak tooth-cavity
Absent

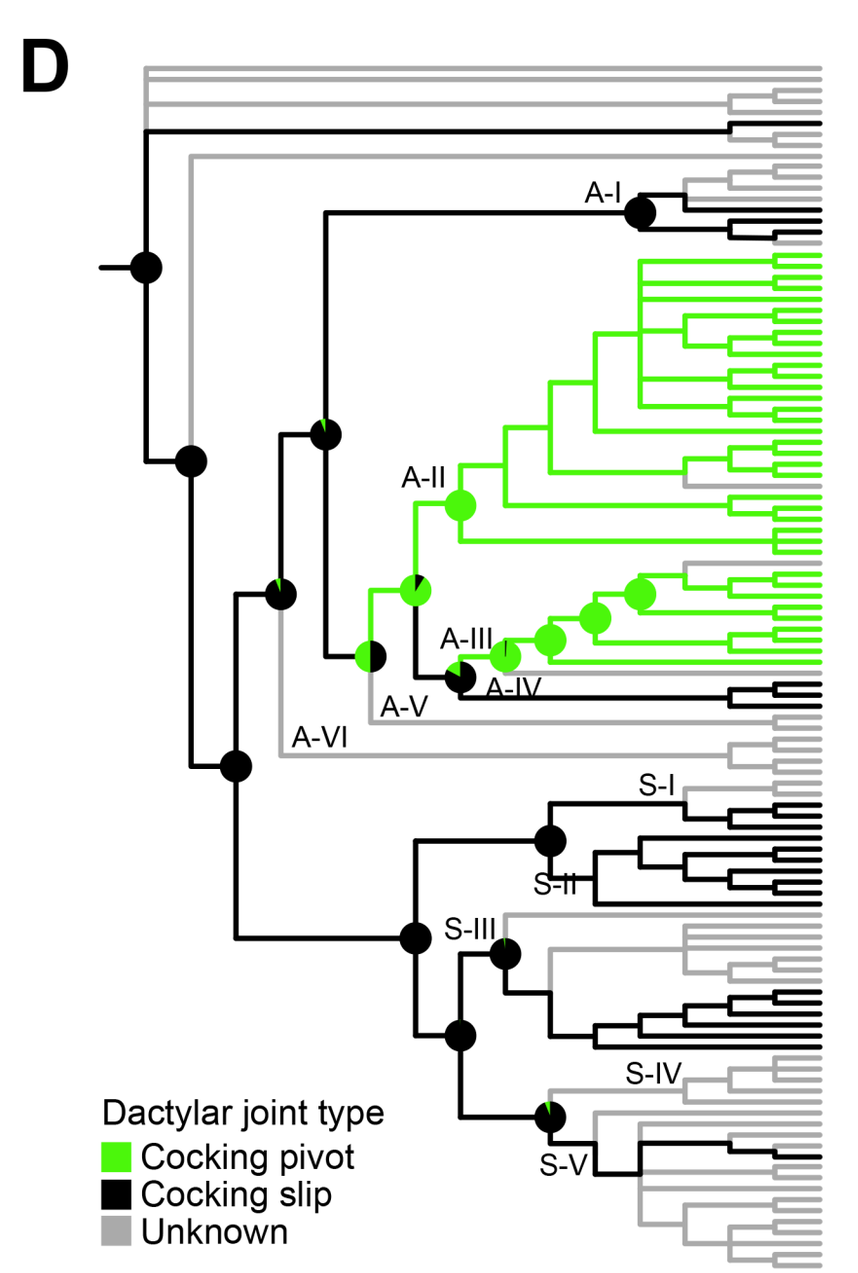
D
A-I
A-II
A-III
A-IV
A-V
A-VI
S-I
S-II
S-III
S-IV
S-V
Dactylar joint type
Cocking pivot
Cocking slip
Unknown

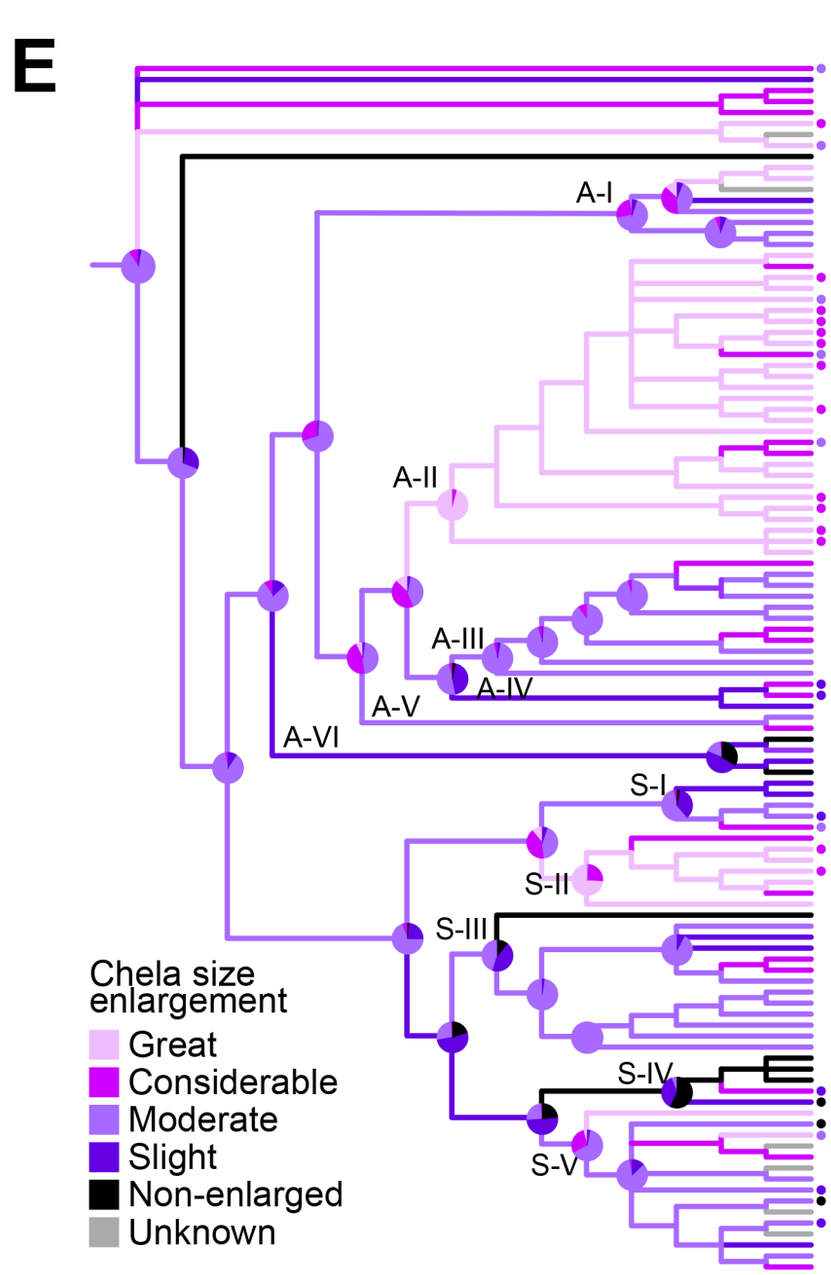
E
A-I
A-II
A-III
A-IV
A-V
A-VI
S-I
S-II
S-III
S-IV
S-V
Chela size enlargement
Great
Considerable
Moderate
Slight
Non-enlarged
Unknown

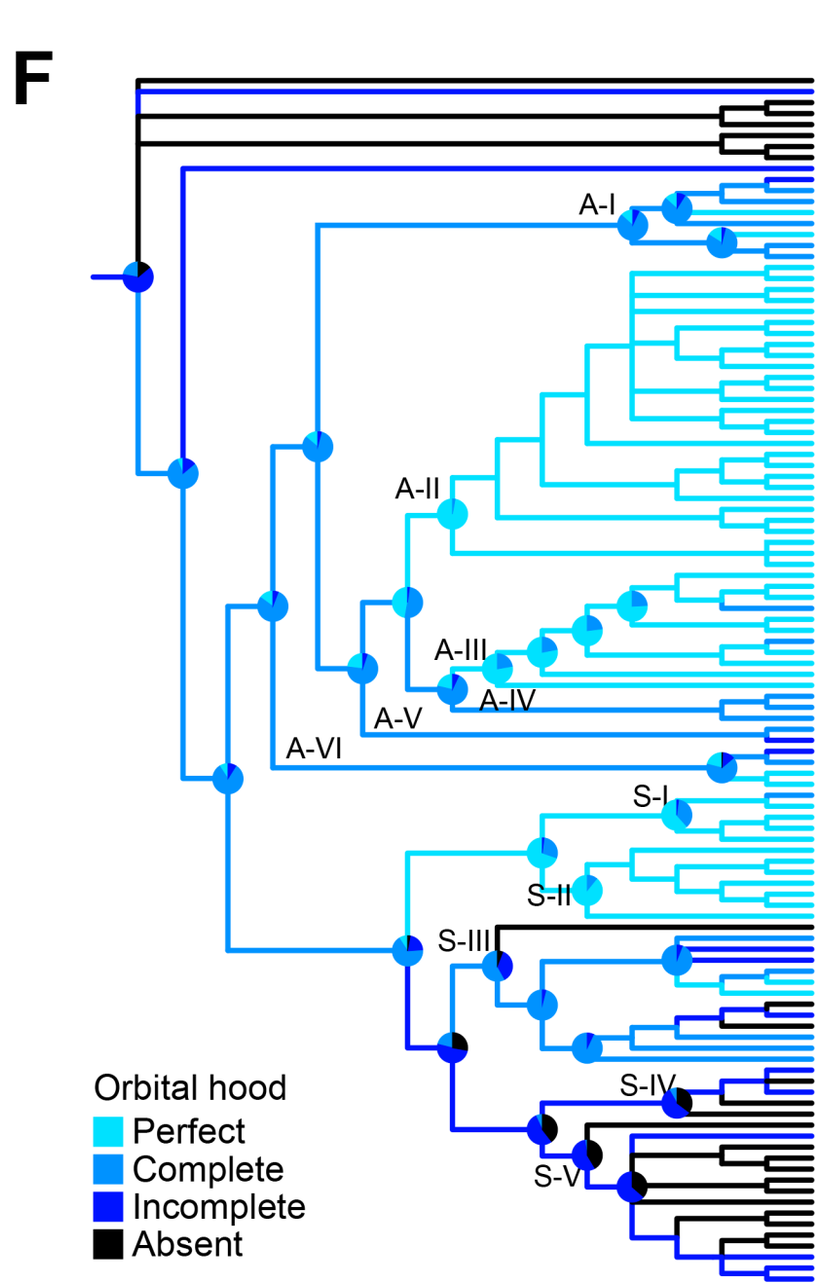
F
A-I
A-II
A-III
A-IV
A-V
A-VI
S-I
S-II
S-III
S-IV
S-V
Orbital hood
Perfect
Complete
Incomplete
Absent

Pre-snapping-gain

Snapping gain

Post-snapping-gain

A Snapping & Adhesive Plaques (AP)

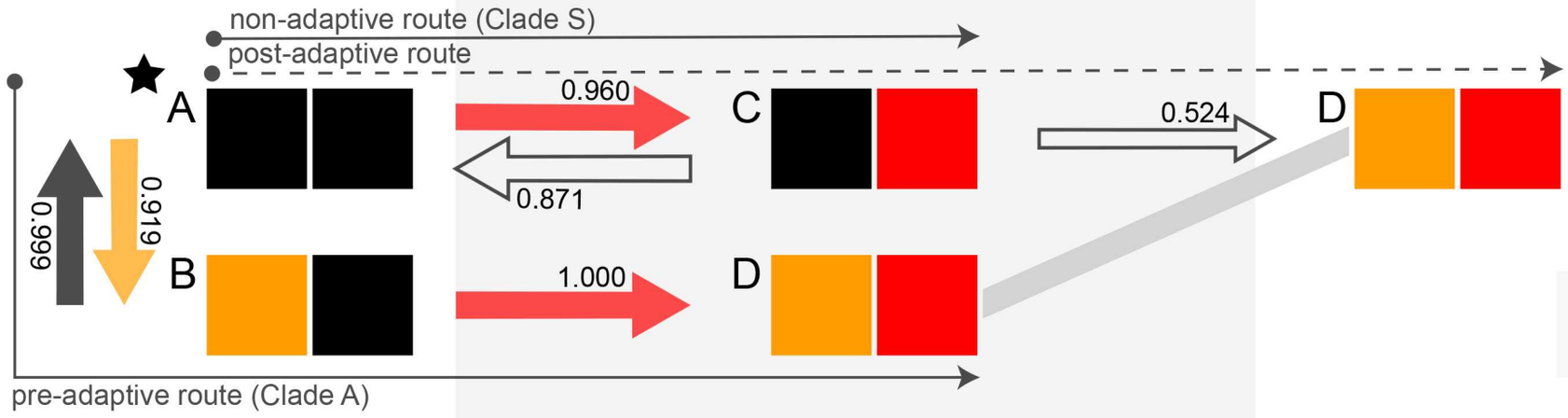

B Snapping & Tooth-cavity (TC) or Cavity-cavity System (CC)

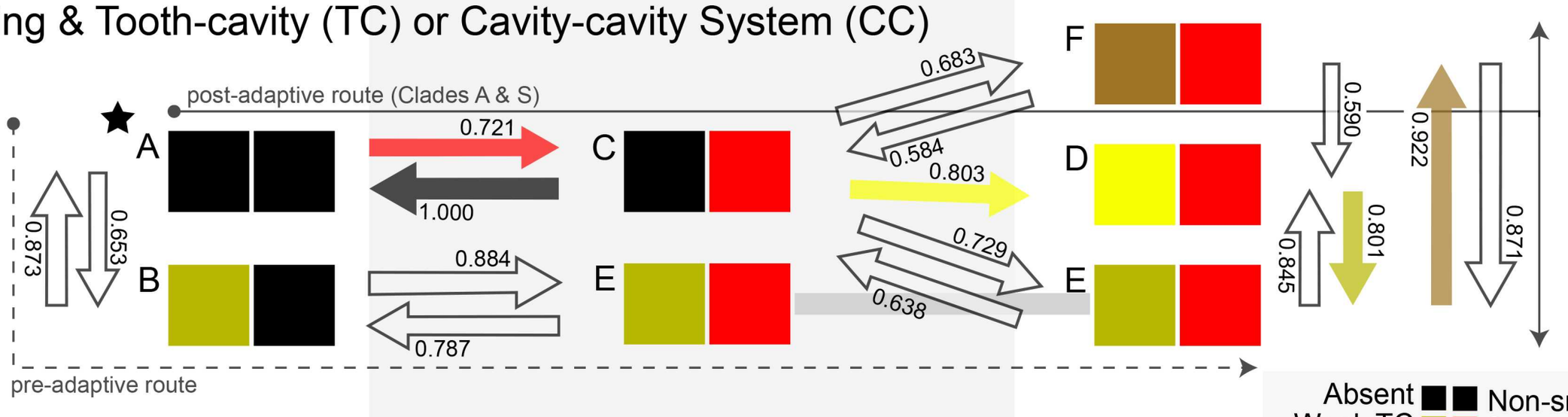

C Snapping & Dactylar Joint

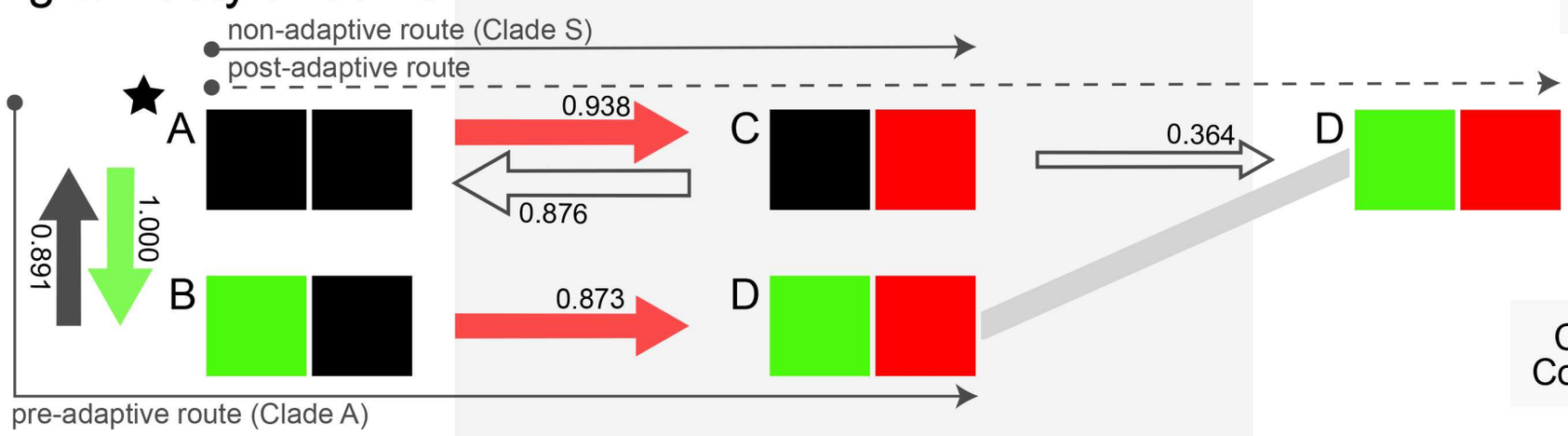

D Snapping & Chela Size Enlargement

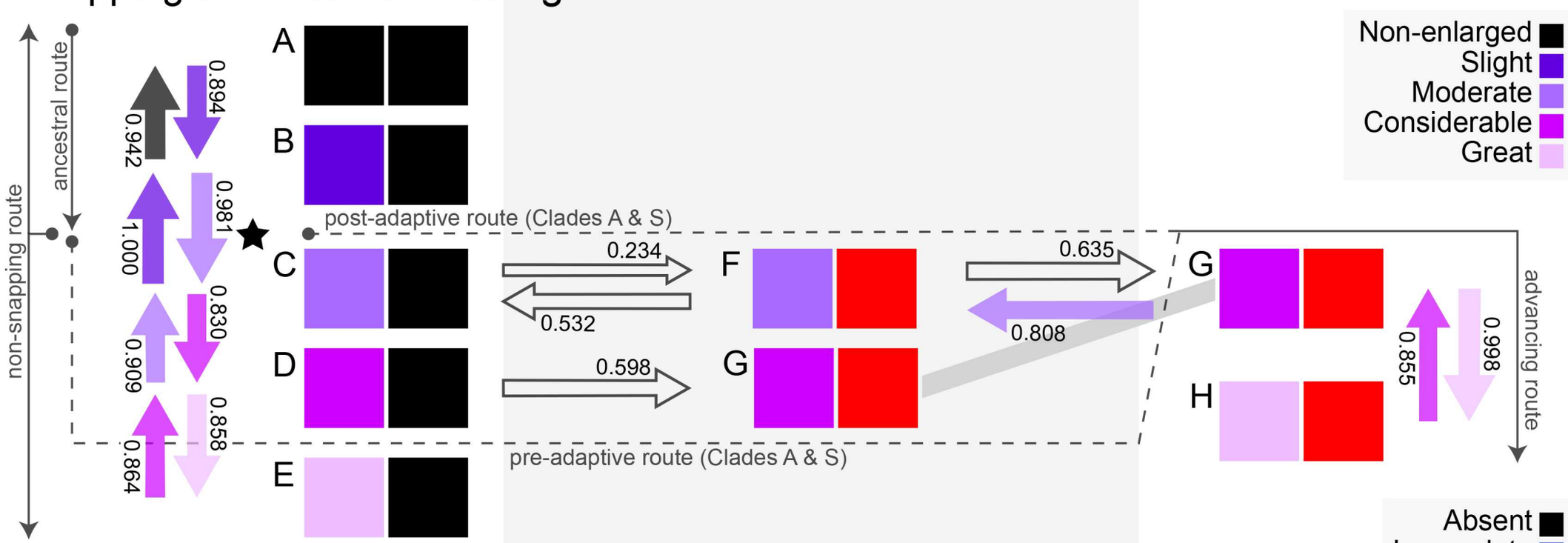

E Snapping & Orbital Hood